



Site characterization report at the seismic station IT.TVL - Tivoli (RM)

Report di caratterizzazione di sito presso la stazione sismica IT.TVL - Tivoli (RM)

Working Group Geology: Luca Minarelli, Massimiliano Porreca, Marta Pischiutta Geophysics: Marta Pischiutta, Giuliano Milana, Fabrizio Cara, Giovanna Cultrera	Date: December 2020
Subject: Final report illustrating the site characterization for seismic station IT.TVL	



<i>Introduction</i>	3
A. Geological setting	3-12
1. Topographic and geological information	3
2. Geological map	5
3. Lithotechnical map	6
4. Survey map	7
5. Geological model	8
5.1 General description	
5.2 Geological section	
5.3 Subsoil model	
B. Vs profile	13-20
1. Geophysical Investigations	13
1.1 Ambient noise HVSR analysis	
1.2 Dispersion curves from passive and active array measurements	
2. Seismic Velocity Model	18
3. Conclusions	21
<i>References</i>	22
<i>Disclaimer and limits of use of information</i>	24



INTRODUCTION

In this report we present the geological setting, geophysical measurements and results obtained in the framework of the 2019-2021 agreement between INGV and DPC, called *Allegato B2: Obiettivo 1 - TASK 2: Caratterizzazione siti accelerometrici (Responsabili: G. Cultrera, F. Pacor)* for the site characterization of station IT.TVL (Tivoli).

Location and coordinates are reported in Table 1.

Table 1.

CODE	NAME	LAT [°]	LON [°]	ELEVATION [m]
IT.TVL	Tivoli	41.89302*	12.77322*	105
ADDRESS	Via di Tivoli, 65, Gallicano nel Lazio (RM) - Italy			

* Reference table from ITACA (December 2020)

A. Geological setting

A1. TOPOGRAPHIC AND GEOLOGICAL INFORMATION

Topographic information related to the site is reported in Table 2.

Table 3 summarizes all available geological maps from literature for geological analyses.

Table 2.

Topography	Description	Topography Class	Morphology Class	EC8 Class
	Flat top of isolated relief with slope $i \leq 15^\circ$	T1	VC*	B

* According to nomenclature of ITACA (December 2020)

**Table 3.**

Geological map	Source	Scale
IT.TVL	Geological map of Italy sheet N.150 (Roma)	1:100.000
IT.TVL	Geological map of Italy sheet N.375 (Tivoli)	1:50.000
IT.TVL	Litho-morphological map – Seismic Microzonation (Gallicano nel Lazio)	1:5.000

In Table 4 Geological and Lithotechnical Units (according to Seismic Microzonation classification; Technical Commission SM, 2015) are described and are concerned to maps of following chapters. The term “original” means the result comes from a pre-existing cartography (Table 3); the term “deduced” means the result comes from an interpretation of a pre-existing cartography according to the nomenclature of corresponding cartography.

Table 4

GEOLOGICAL UNITS		LITHOTECHNICAL UNITS	
Geological map. According to Geological map of Italy 1:50.000 - sheet N.375 (Tivoli). <i>Original</i> .		Lithotechnical Map. According to the nomenclature of Seismic Microzonation (Technical Commission SM, 2015). <i>Deduced</i> .	
code	description	code	description
SFTba	Alluvial deposits	SMtf	Silty sands, mixed of sand and silt of fluvial terrace
VSN2	Villa Senni Form. - Pozzolanelle	GMig	Silty gravel, mixed gravel, sand and silt of ignimbrite deposits
VSN1	Villa Senni Form. - Tufo Lionato	GR	Cemented granular
SLVb	Fontana Centogocce Form. - pyroclastites	GMsc	Silty gravel, mixed gravel, sand and silt of volcanic slag
PNR	Pozzolane Nere	GMig	Silty gravel, mixed gravel, sand and silt of ignimbrite deposits
RED	Pozzolane Rosse	GMig	Silty gravel, mixed gravel, sand and silt of ignimbrite deposits



A2. GEOLOGICAL MAP

In Figure 1 Geological Map is reported in a 1km x 1km square around the station.

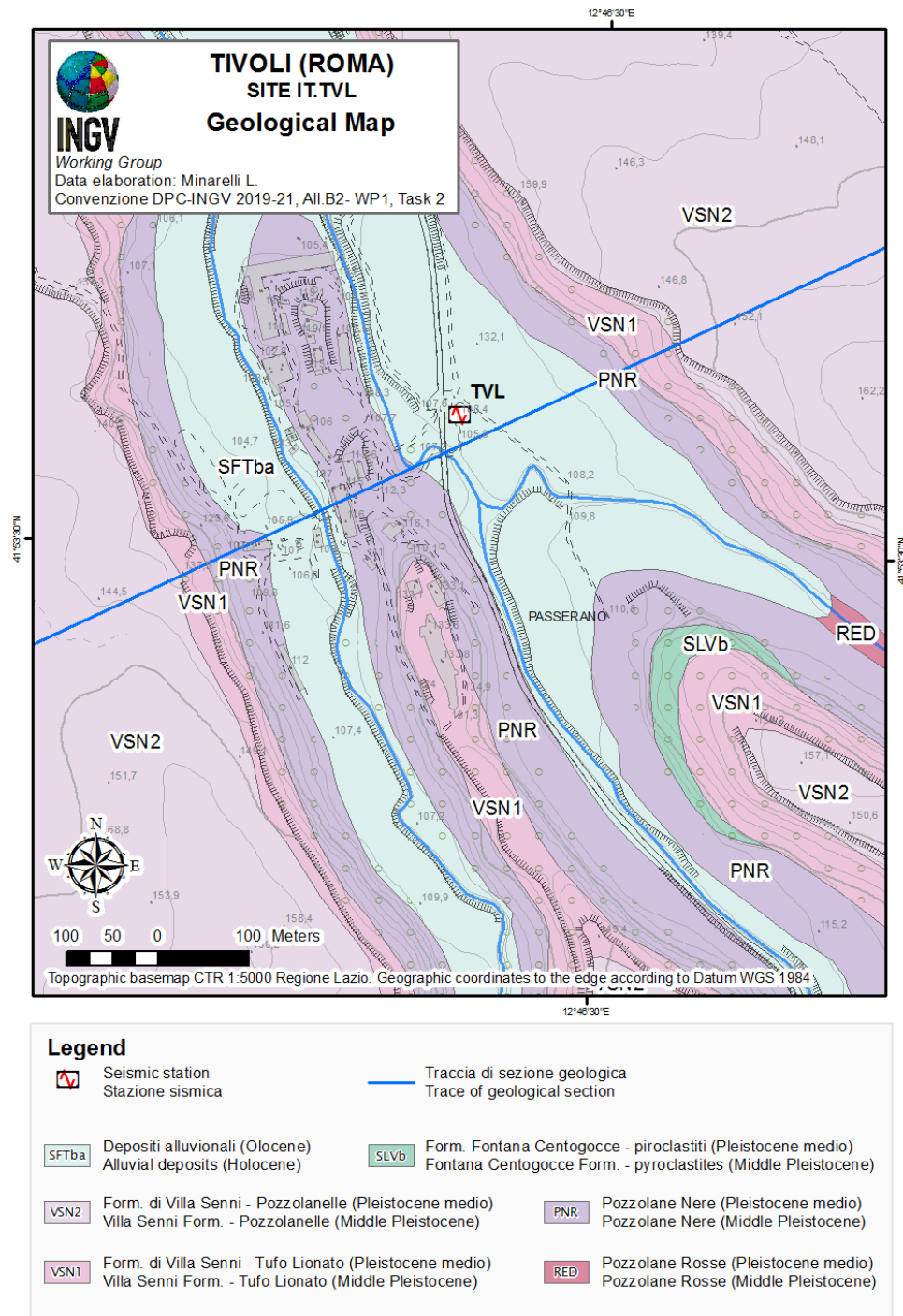


Figure 1. Geological map of seismic station site IT.TVL - scale 1:5.000. Geological units are mapped according to the nomenclature of geological map of Italy 1:50.000 - sheet N.375 (Tivoli).



A3. LITHOTECHNICAL MAP

In Figure 2 Lithotechnical Map is reported in a 1km x 1km square around the station.

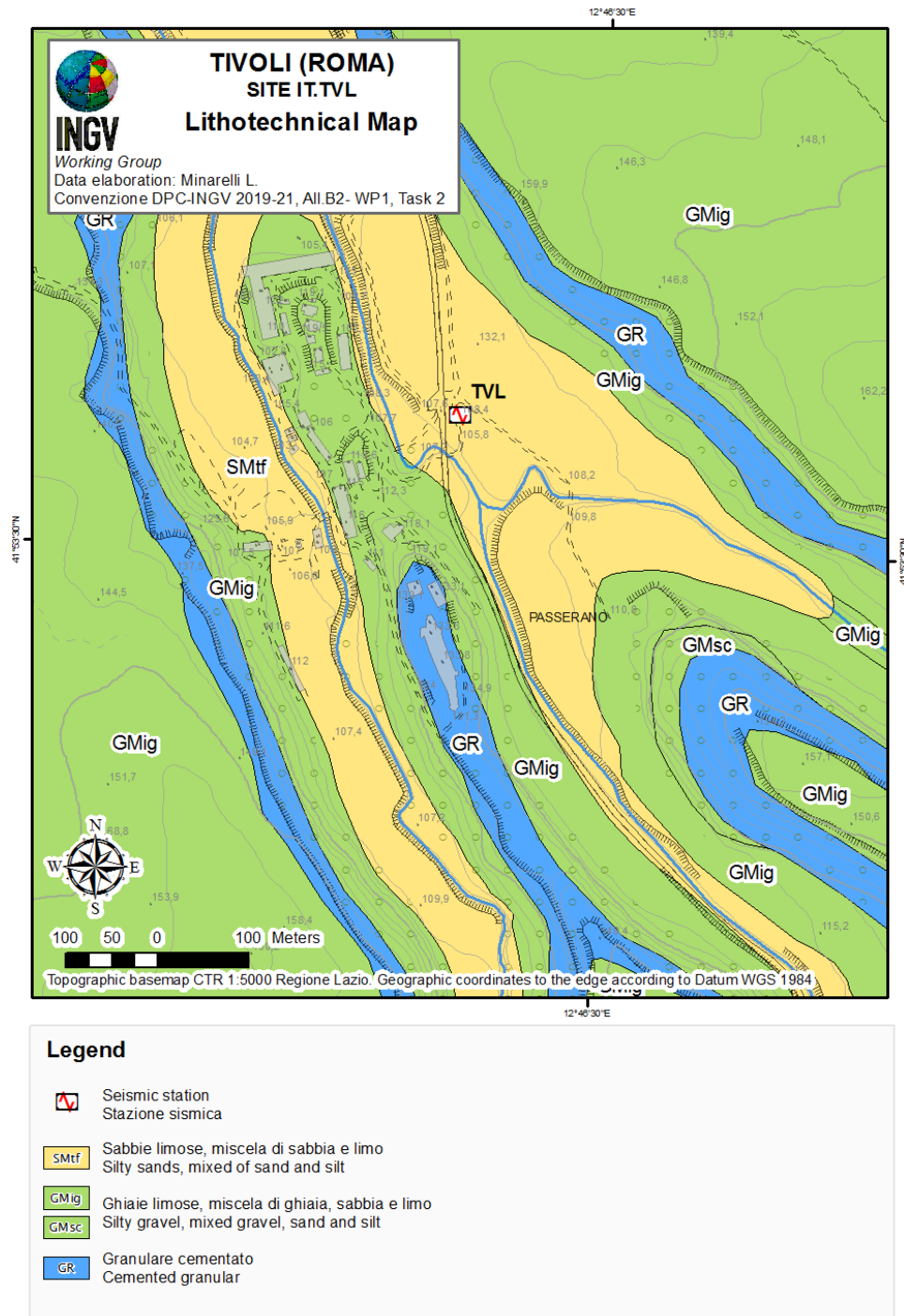


Figure 2: Lithotechnical map of the seismic station site IT.TVL - scale 1:5.000. The lithotechnical units are attributed according to the nomenclature of Seismic Microzonation study (Technical Commission SM, 2015).

Convenzione DPC-INGV 2019-21, All.B2- WP1, Task 2: "Caratterizzazione siti accelerometrici" (Coord.: G.Culturra, F. Pacor)

Cite as: Working group INGV "Agreement DPC-INGV 2019-21, All.B2- WP1, Task 2", (2020). Site characterization report at the seismic station IT.TVL - Tivoli (RM) <http://hdl.handle.net/2122/14053>



A4. SURVEY MAP

Figure 3 shows the Survey Map reporting both previous investigations and geophysical surveys conducted by INGV Working Group.

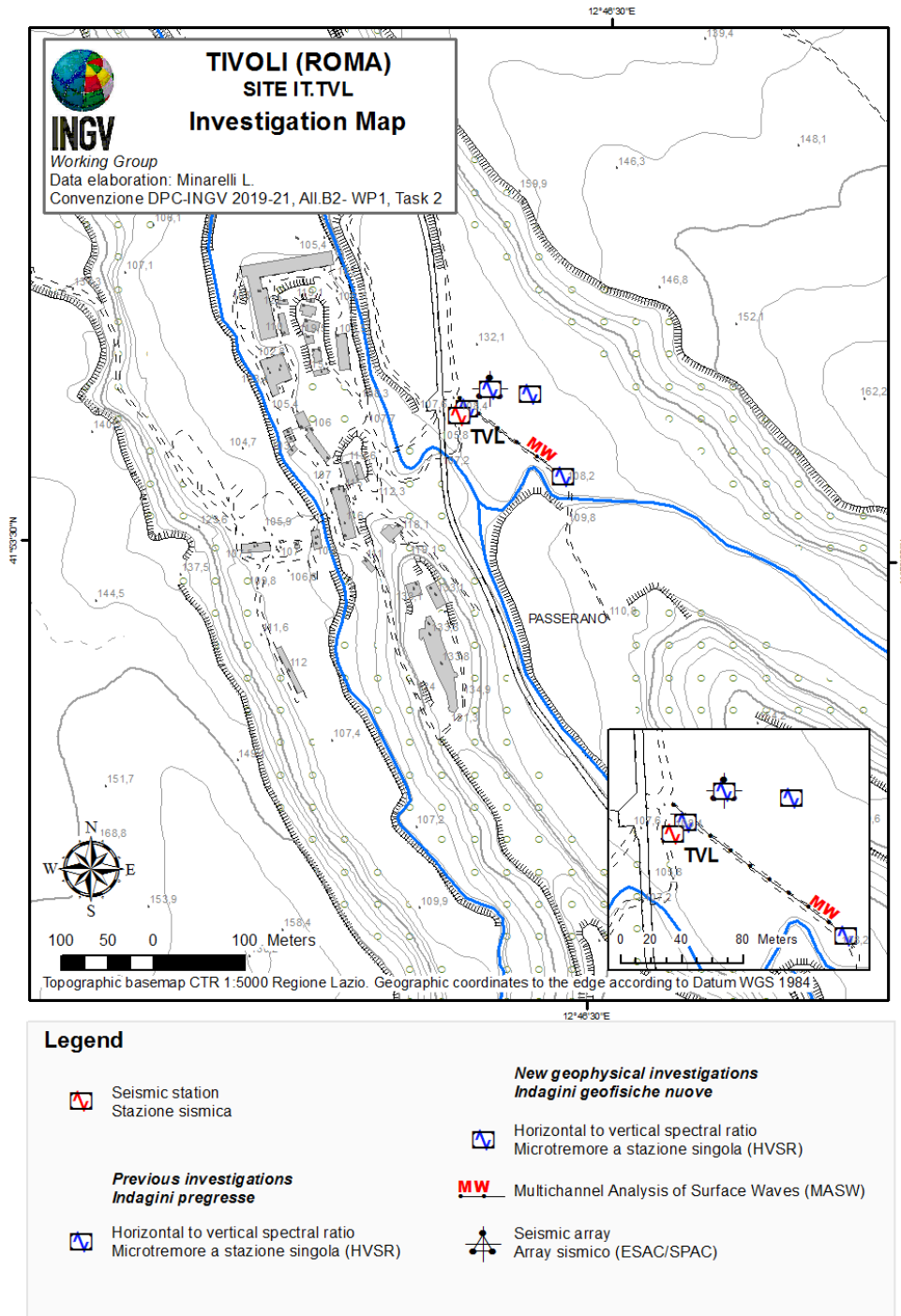


Figure 3: Map of the geophysical surveys made in the sectors around the seismic station IT.TVL - scale 1: 5.000. The box at the bottom right contains a zoom of the area with the detail of the geophysical investigation conducted by INGV Working Group for the seismic characterization of the site (Convenzione DPC-INGV 2019-21, Allegato B2-WP1, Task B, Velocity profile at the seismic station report IT.TVL).

Convenzione DPC-INGV 2019-21, All.B2- WP1, Task 2: "Caratterizzazione siti accelerometrici" (Coord.: G.Culturra, F. Pacor)

Cite as: Working group INGV "Agreement DPC-INGV 2019-21, All.B2- WP1, Task 2", (2020). Site characterization report at the seismic station IT.TVL - Tivoli (RM) <http://hdl.handle.net/2122/14053>



A5. GEOLOGICAL MODEL

5.1 General description

The investigated area is located along the Tyrrhenian border of Lazio mountain chain, between the northern slopes of the Colli Albani volcano and those of the first Apennine reliefs, the Prenestini and Tiburtini Mountains.

The tectonic structure of the Tyrrhenian Latium margin is dominated by high-angle normal faults, striking in a NW-SE direction. The faults are related to the Plio-Pleistocene extensional tectonics, associated with the opening of the Tyrrhenian Sea. The faults are well visible and seismically active in the Apennine chain area, whereas, they are generally buried under the extensive Quaternary volcanic covers, along the Tyrrhenian edge.

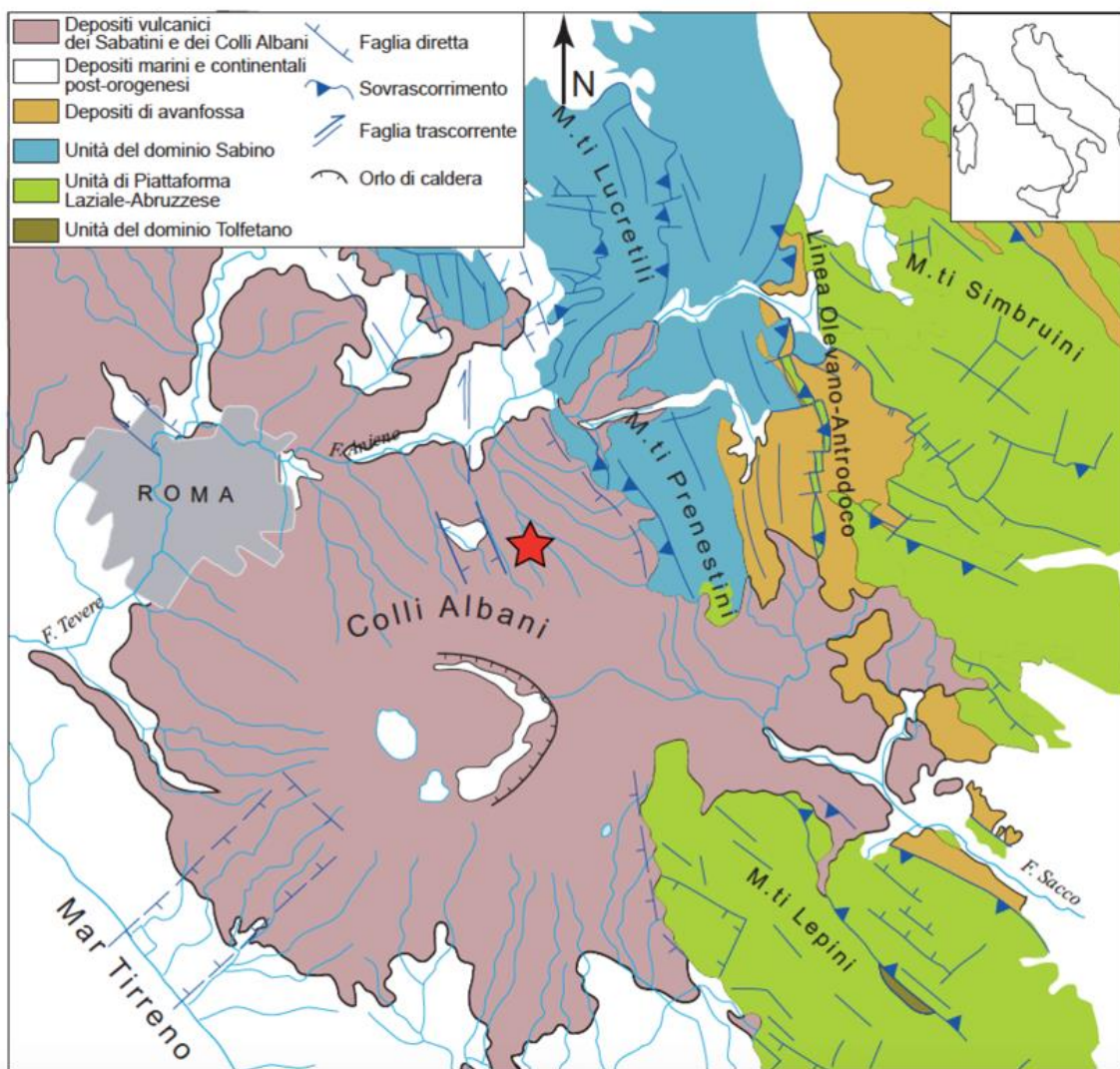


Figure 4: Structural scheme of the Tyrrhenian margin of Latium. The red star depicts the study site.
<https://www.socgeol.it/N2042/23-giugno-2019-il-terremoto-di-colonna-la-sismicità-alle-porte-di-roma.html>

Convenzione DPC-INGV 2019-21, All.B2- WP1, Task 2: "Caratterizzazione siti accelerometrici" (Coord.: G.Cultrera, F. Pacor)

Cite as: Working group INGV "Agreement DPC-INGV 2019-21, All.B2- WP1, Task 2", (2020). Site characterization report at the seismic station IT.TVL - Tivoli (RM) <http://hdl.handle.net/2122/14053>



The first and most intense eruptive phase of the Albano Volcano took place between 600 and 350 thousand years ago (De Rita et al., 1995) and induced the accumulation of large thicknesses of mainly ignimbrite rocks, interbedded with lava expansions and with fallout and reworking rocks.

The lower portion of the ignimbrite succession shows a marked phreatomagmatic character and is framed into the Volcano Laziale Lithosome (Funiciello & Giordano, 2010; Giordano et al., 2006, 2010).

The Lithosome outcrops extensively all around the more recent Albano caldera, forming a large tabular plateau, characterized by very low slopes (2° - 5°) and deep-sided river valleys, eroded during the Wurmian synglacial lowstand of sea level.

Just to the west of the investigated area, the surface of the ignimbrite plateau is affected by the circular depressions of the Prata Porci, Pantano Secco, and Castiglione maars and by the large morphotectonic depression, of the Pantano Borghese, associated with synvolcanic direct faults, striking in a NNW-SSE direction.

The north-eastern edge of the ignimbrite plateau corresponds to the first slopes of the Prenestini Mountains, where Apennine units similar to the Umbro-Marchigiana successions outcrop, consisting of Liassic carbonate platform limestones, Jurassic and Cretaceous slope and basin deposits, escarpment and Tertiary carbonate and terrigenous deposits. Similar units were recognized below the so-called “post-orogenic” terrigenous sedimentary deposits of the early Pleistocene and the Quaternary volcanic activity of the Alban Hills (e.g. Gallicano area, Funiciello & Parotto, 1978; Danese & Mattei, 2010).

5.2 Geological Section

The seismic station is located near the village of Passerano, within a deep, narrow valley, incised during the last Wurmian glacial lowstand of sea level.

In order to describe the geologic structure of the study area, a geologic section was drawn (Figures 1 and 5), crossing the IT.TVL site, based on published cartographic information from the CARG and Seismic Microzonation geological surveys. The correlation with subsurface geognostic data is quite poor being based on a single well, drilled in the close Prenestina highway service area, about 1 km west far from the study area.

On the valley walls, some of the ignimbrite units generated by the large volume eruptions of the Vulcano Laziale complex outcrop extensively. The volcanic succession has a mainly tephriphonolitic composition. Its upper portion is formed by massive and chaotic, coarse-ash to fine-lapilli, matrix-supported, purple to black, unconsolidated ignimbrites, with up to 30% of coarse lapilli- to block-sized lava fragments and xenoliths of intrusives.

The unit is called Pozzolanelle (VSN2 - *Pozzolanelle Auctt.*) and shows a maximum thickness of 20 meters, forming the upper part of the Lithosome of the Vulcano Laziale.

The Pozzolanelle unit rests on massive and chaotic, ash matrix-supported, zeolite lithified, yellow to red ignimbrites, with yellow pumice and grey scoria lapilli (VSN1 - *Tufo Lionato*



"litoide" Auctt), about 10 meters thick. Both the Tufo Lionato and the Pozzolanelle units are framed within the Villa Senni Formation, of Middle Pleistocene age.

In the lower portion of the valley cliff, about 25 meters of massive and chaotic, ash matrix supported, black, unconsolidated ignimbrite outcrops, with up to 10% of coarse lapilli- to block-sized volcanic, thermometamorphic, and intrusive xenoliths. Part of the Passerano village was built on the ridge cut into this ignimbrite unit, called Pozzolane Nere (PNR).

The valley floor is formed by alluvial terraces, eroded into Holocene deposits (SFTba), consisting of alternating sands, silts, and clays.

The buried part of the volcanic succession has been reconstructed with a high degree of uncertainty, due to the lack of stratigraphic investigation crossing the deepest portion of the sedimentary succession. The proposed reconstruction was based just on a single well, drilled in the Prenestina highway service area. Below the Pozzolane Nere unit, the well shows about 10 meters of unconsolidated dark tuffs, followed by a few meters of black lavas. These rocks, which cannot easily be correlated, may be laterally absent, due to erosion or non-deposition.

Below these rocks, there are again massive and chaotic, coarse-ash matrix-supported, red, purple to dark grey, unconsolidated ignimbrites, with coarse lapilli to block sized volcanic, thermometamorphic, and intrusive xenoliths. These ignimbrites can be correlated with the Pozzolane Rosse unit (RED), according to their stratigraphic position. The presence of the Pozzolane Rosse below the Pozzolane Nere is also confirmed by their extensive outcropping in neighbouring areas, where the direct contact between the two units is visible.

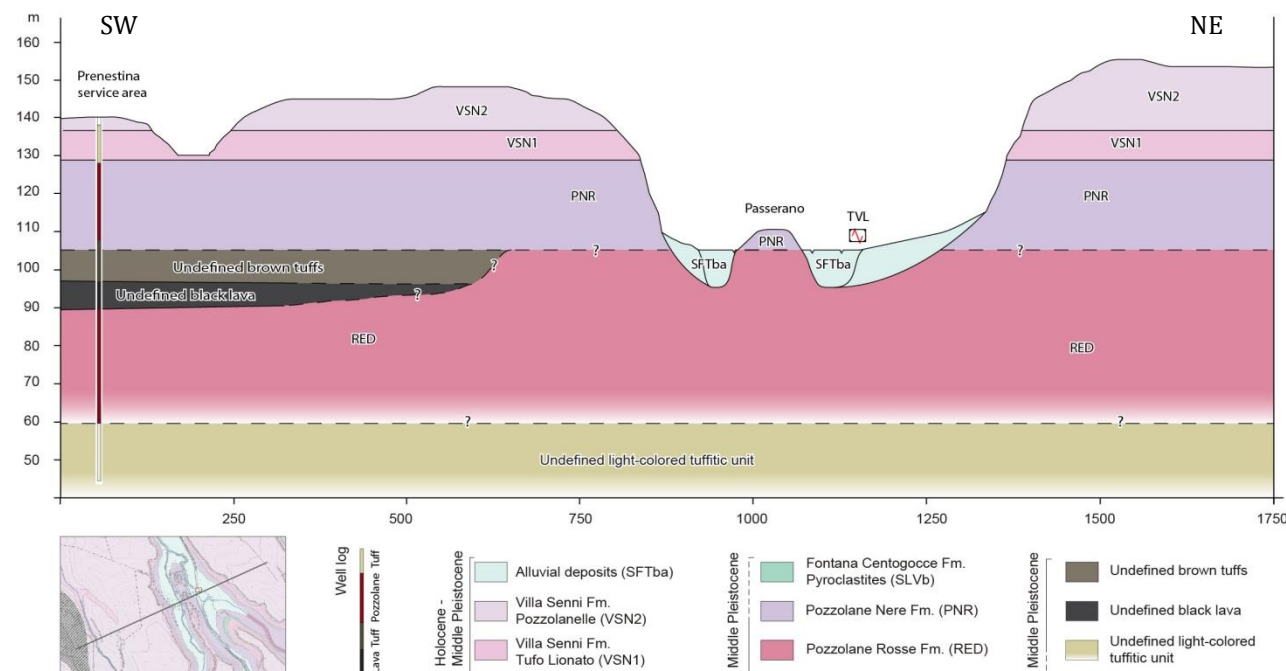


Figure 5: Schematic geological cross section, oriented SW-NE, showing the relationships between the Pleistocene ignimbrite units and the Holocene sedimentary infilling of incised valley.



At the base of the geologic section, an undefined light-colored tuff unit has been indicated, based on the well stratigraphy at the Prenestina service area. These tuffs, probably lithoid in nature, are most likely connected to the oldest phase of the phreatomagmatic eruptive activity of the Vulcano Laziale.

5.3 Subsoil model

A model to the depth of 60 meters was developed for the area surrounding the IT.TVL station (Figure 6). The model is based on extrapolation of surface data and subsurface information deriving from a single well and the new geophysical investigations performed by the INGV Working Group for the seismic characterization of the site and the definition of the velocity profiles of the seismic body waves. The subsurface model cannot therefore be well constrained and the thicknesses of stratigraphic units can only be estimated. The thickness of the Holocene alluvial covers below the valley floor has been estimated to about 10 meters, according to the Seismic Microzonation study of the Municipality of Gallicano nel Lazio.

The reconstructed geometric relationships seem to indicate that, at the station site, the Holocene alluvial deposits (SFTba) are in direct contact with the underlying Pozzolane Rosse (RED).

The thickness of the ignimbrite succession framed into the Pozzolane Rosse has been estimated to at least 30 meters, based on the same single well data. Such values agree with those reported by literature for this unit.

Below the Pozzolane Rosse, an undefined light-colored tuff interval is indicated. The information from well stratigraphy and geophysical measurements, realized for the seismic characterization of the station site, indicates that the tuffs are most probably of lithoid consistency.

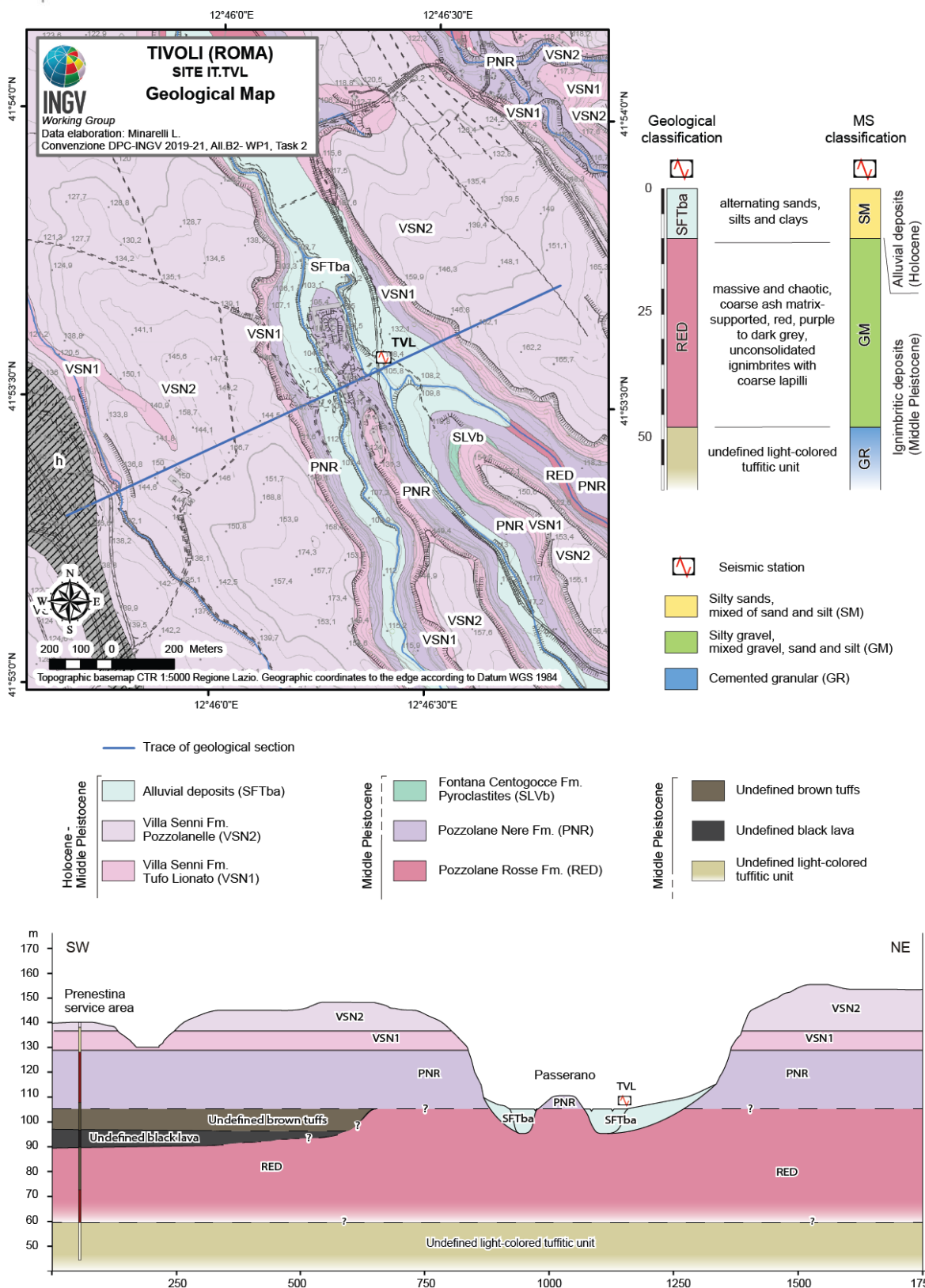


Figure 6: Bottom - Geological section crossing seismic station IT.TVL. Right - Subsoil model under the IT.TVL seismic station and classification according nomenclature of geological map of Italy 1:50.000 and according to Seismic Microzonation (SM).

Convenzione DPC-INGV 2019-21, All.B2- WP1, Task 2: "Caratterizzazione siti accelerometrici" (Coord.: G.Culturra, F. Pacor)

Cite as: Working group INGV "Agreement DPC-INGV 2019-21, All.B2- WP1, Task 2", (2020). Site characterization report at the seismic station IT.TVL - Tivoli (RM) <http://hdl.handle.net/2122/14053>



B1. GEOPHYSICAL INVESTIGATIONS

Geophysical investigations were performed in the area surrounding the seismic permanent station IT.TVL, with the aim of defining a 1D-velocity model. We carried out active and passive measurements placing vertical geophones following a linear and a spiral-shape array, respectively. We installed also 3 temporary seismic stations to record ambient noise.

Figure 7 shows the location of the two arrays and temporary seismic stations deployed in the target area around the IT.TVL station (red triangle).



Figure 7. Plan view of geophysical measurements performed in the surroundings of permanent station IT.TVL (yellow circle): active linear array (red line), passive spiral-shape array (green circles depicting the position of vertical geophones), and temporary seismic stations recording ambient noise (blue triangles).

The geophysical investigations were performed in the cultivated field adjacent to the IT.TVL seismic station (Figure 7). The conditions were favourable to easily deploy both linear and a spiral-shape arrays. For the former we used an existing clay pathway where we set 48 vertical 4.5 Hz geophones, equally spaced of 3 m, for a total profile length of 141 m. The spiral-shape array was performed using 24 vertical 4.5Hz geophones following two concentric circles with approximate radius of 10 and 25 m. We also installed 3 temporary seismic stations equipped with Lennartz Marslite digitizers renewed by Sara Electronics and Lennartz-5s sensors.

Convenzione DPC-INGV 2019-21, All.B2- WP1, Task 2: "Caratterizzazione siti accelerometrici" (Coord.: G.Cultrera, F. Pacor)

Cite as: Working group INGV "Agreement DPC-INGV 2019-21, All.B2- WP1, Task 2", (2020). Site characterization report at the seismic station IT.TVL - Tivoli (RM) <http://hdl.handle.net/2122/14053>



During the measurements the weather conditions were favourable, e.g. day without wind and rain. Figure 8 shows some pictures taken during the survey. The position of geophones and seismic stations was accurately measured through a differential Leika GPS.

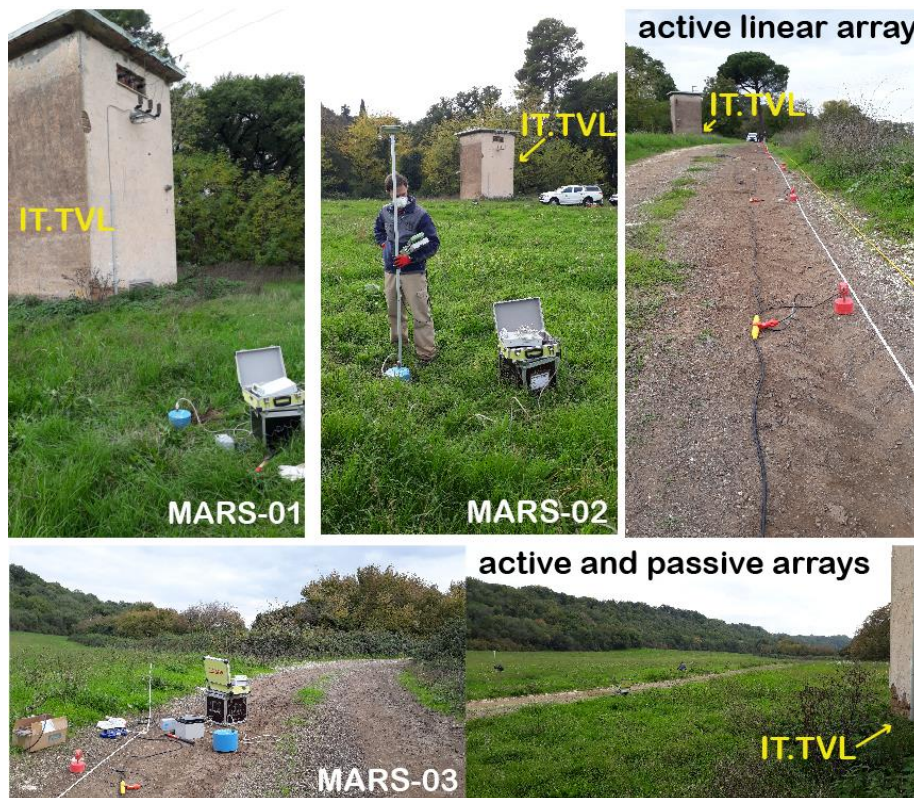


Figure 8. Pictures taken during the survey representing the three noise measurements (MARS-01, 02 and 03), the linear and spiral-shape arrays. The site hosting the IT.TVL permanent seismic station is indicated too.

B1.1 Ambient noise HVSR analysis

The temporary seismic stations MARS-01 and MARS-02 acquired ambient noise for about 3h40m and 1h20m, respectively. Unfortunately, station MARS-03 did not work properly and a relevant part of the recording is missing. We therefore could not process its data.

On the former two stations we calculated HVSR (Horizontal-to-Vertical Spectral Ratios), by applying an antitrigger algorithm to select the most stationary part. Signals were smoothed using a Konno-Ohmachi filter (Konno and Ohmachi, 1998), and a 5% cosine taper was applied. The HVSRs calculated as the geometric mean of the two horizontal components are shown in Figure 9. Results at the two stations are generally in good agreement, the HVSR showing a clear peak at about 4 Hz (3.9 and 3.7 for MARS-01 and MARS-02). While at station MARS-01 this peak is narrower and has a more regular shape, at station MARS-02 it seems to be composed by two different semi-superimposed peaks. These slight differences may be caused by tiny lateral variations in the alluvium thickness and/or velocity. In Figure 10 we also show spectra calculated separately for the three components of motion. Between 2 and 6 Hz, in the amplified frequency band, they form a lozenge-shape, confirming the consistency of



the HVSR peak. This observation leads to exclude that it might be caused by a deamplification of the vertical component. In this frequency band, the two horizontal components show comparable amplitude values, also suggesting the absence of directional amplification. This is evident also in Figure 11, where we plot as a contour map the HVSRs calculated after rotating the two horizontal components by steps of 10° , from 0° to 180° : the y-axis represents the rotation angle (azimuth in degrees from geographic North), and amplitudes are expressed by a color scale.

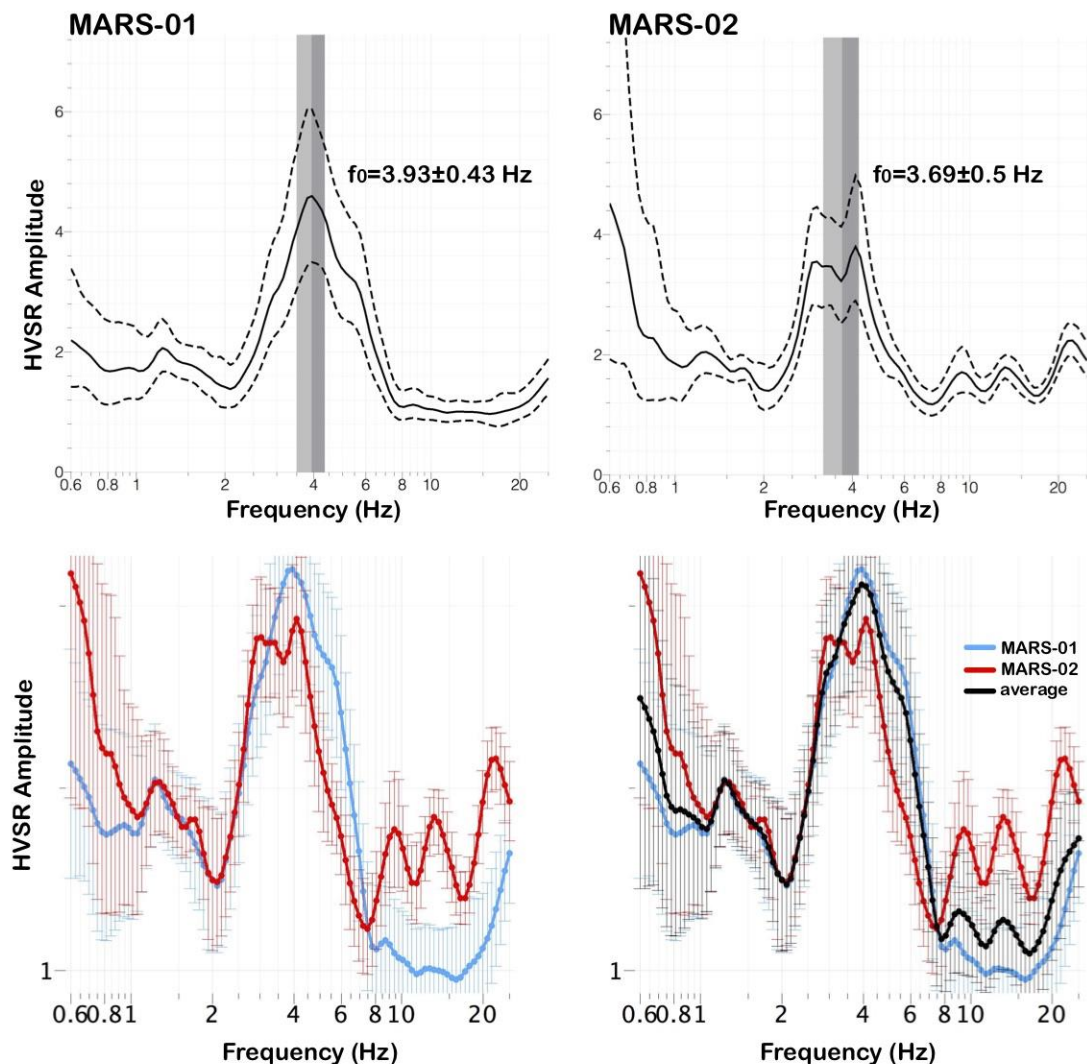


Figure 9. (top) HVSR at temporary stations MARS-01 and MARS-02, calculated on ambient noise recording as the geometric mean of the two horizontal components. The peak value for f_0 is also reported, as well as its associated standard deviation. (bottom) HVSR at the two stations

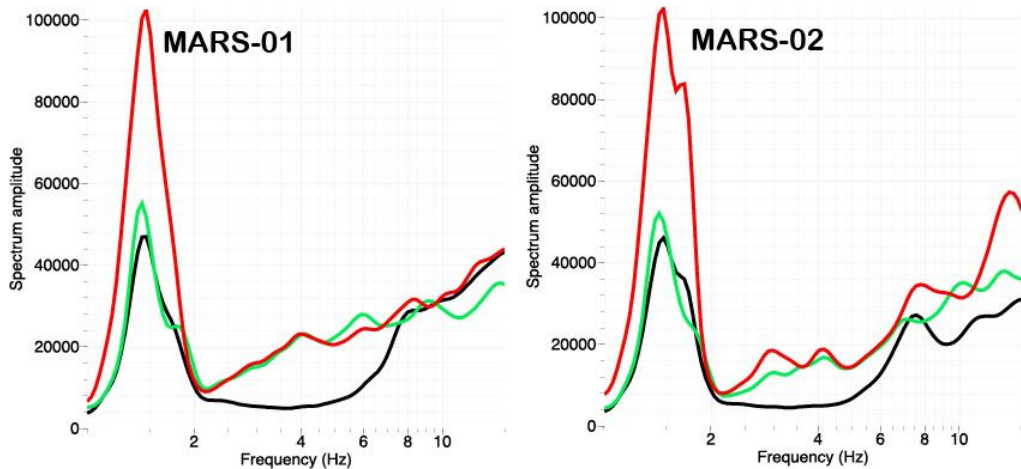


Figure 10. Individual spectra of the vertical (black) and the two horizontal components (NS=green, EW=red).

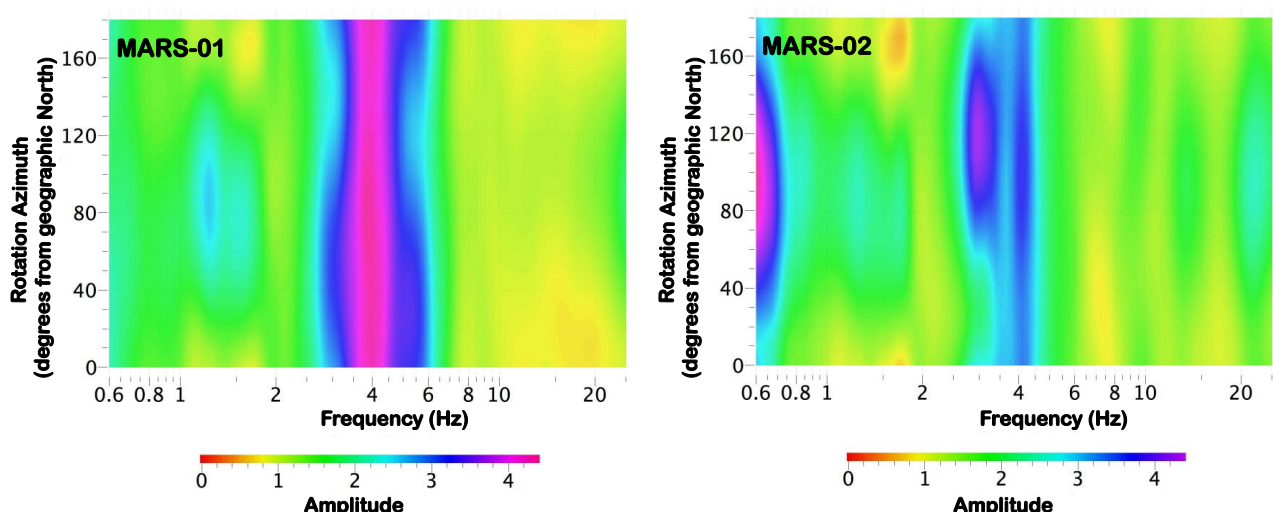


Figure 11. H/V spectral ratios at temporary stations MARS-01 and MARS-02, obtained after rotating the two horizontal components by steps of 10°, from 0° to 180°.

B1.2 Dispersion curves from passive and active array measurements

In the linear array configuration, the 48 vertical geophones were deployed along a straight line with a regular spacing of 3 m. For the MASW analysis, we acquired the seismic signals produced by the impact of a 5 kg hammer on the ground. Shots were made at the following distances (offset) from the position of the first geophone, located in the NW portion of the profile (considered at 0 m): -15 m, -2 m, 70.5, 143 m and 156 m. In order to increase the signal-to-noise ratio we performed three shots for each position. The seismic data were acquired using two multichannel systems (Geode manufactured by Geometrics, each of which manages 24 channels) with a sampling rate of 0.125 ms for a duration of 2 s.

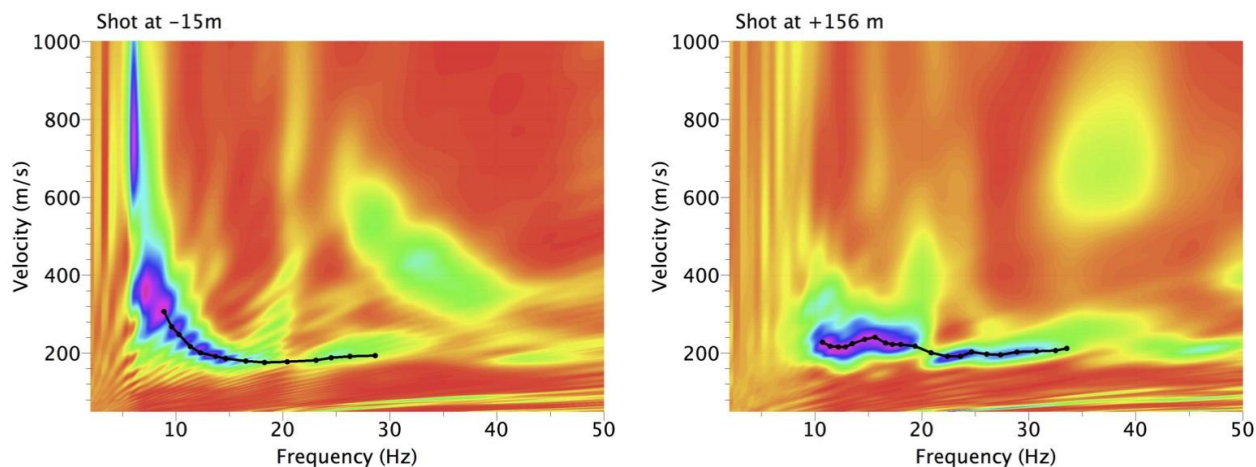


Figure 12. FK analysis. The results obtained by MASW linear array shot are shown for each shot; from top to down the offset is -10 m, -5 m, -2 m, 34.5 m, 73 m, 76 m and 81m. Plots in the same horizontal panel refer to the same shot offset location and the black curves lines represent the picked dispersion curve.

The acquired data were processed using the *GEOPSY* software (www.geopsy.org), in order to extract the surface-wave dispersion properties of subsoil by applying frequency-wavenumber (FK) analysis to the seismic signals. Figure 12 shows results obtained for shot points at 15 m from the first and last geophones, respectively, for which we could identify and manually peak a dispersion curve. The differences in the dispersion curves, mostly between 10 and 20 Hz, suggest the presence of lateral velocity heterogeneity and lateral heterogeneity in the alluvial sediments. Unfortunately, at the other shot points we obtained low-quality results being impossible to pick any dispersion curves.

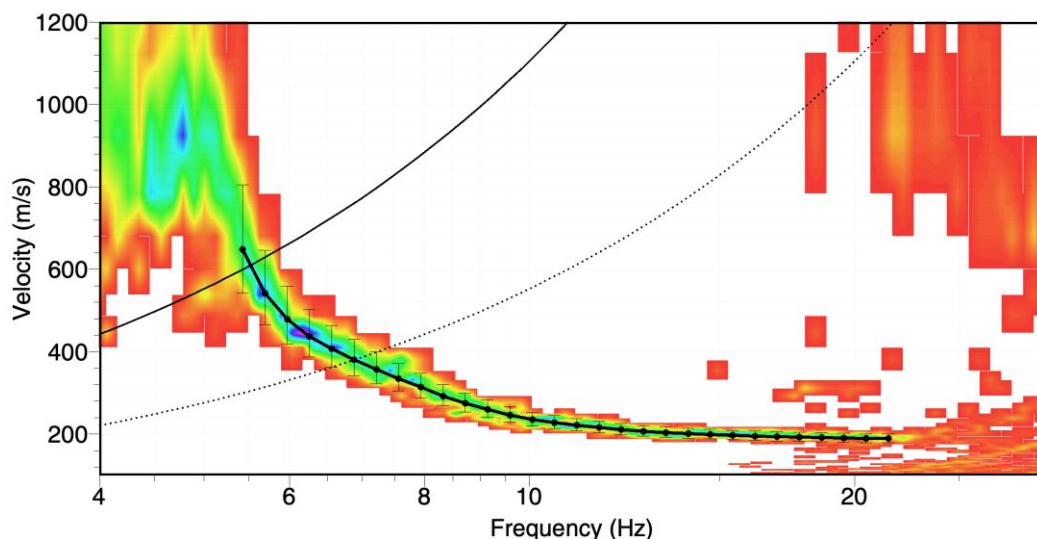


Figure 13. FK analysis applied to passive measurements acquired by the spiral-shape array. The picked dispersion curve along with the standard deviation is plotted. The hyperbolic solid represents the wave-number (K_{max}) limit of the array, whereas the dotted curve is a more careful limit ($K_{\text{max}}/2$).



In the spiral-shape configuration, the 24 vertical geophones were deployed following two roughly concentric circles with radius of 10 and 25 m, respectively (see Figure 7). They acquired ambient noise for 1h10m using one of the same multichannel systems previously described (Geode manufactured by Geometrics) with a sampling rate of 4 ms. Again, the acquired data were processed using the *GEOPSY* software (www.geopsy.org), in order to extract the surface-wave dispersion curve through the frequency-wavenumber (FK) analysis. We obtained a well-defined dispersion curve between about 5.5 and 21.5 Hz (Figure 13).

The dispersion curves from MASW linear array and the spiral-shape array have a similar shape but differ in the velocities. This behaviour can be due to the compaction of the road where the linear array was deployed in comparison with the worked soils where the spiral array was set. Considering such differences as well as the different behaviour observed at the opposite sides of the linear array (Figure 12), the impossibility to peak a dispersion curve for the most part of shot points in the linear array, and the highest quality and definition at low frequency of the dispersion curve retrieved from the spiral-shape array, we finally chose to use only this latter in the following inversion procedure. Because down 6Hz the velocities increase very quickly and with more uncertainties (Figure 13), we prefer to cut the dispersion curve from 6Hz to 21.5Hz.

B2 SEISMIC VELOCITY MODEL

In order to derive a seismic velocity model, we performed a joint-inversion using the GEOPSY tool *dinver*, considering as targets the dispersion curve obtained from the spiral-shape array and the HVSR curve at station MARS-2 (located in the center of the array). To proceed with the inversion step, the dispersion curve derived from the vertical component of motion was associated with the fundamental mode of surface Rayleigh-wave. The inversion processing uses the Neighbourhood Algorithm (Sambridge, 1999; Wathelet et al., 2005).

We tested several simple starting model-parameterization finally choosing to use a superficial layer with mechanical properties increasing with depth, and two uniform layers over half-space, keeping in mind the limited depth of investigation associated with the geometry of the array (about 30-50mt). The HVSR curve allows constraining the model with the most important impedance contrast.

Shear wave velocities (V_S) were set to vary for the four layers within the ranges of: 100-300 m/s in the 1st layer; 150-500 m/s in the 2nd layer; 150-700 m/s in the 3rd layer; 150-1500 m/s in the final half-space. Compression wave velocities (V_P) were linked to V_S via the Poisson's ratio (between 0.3 and 0.45) and were set to vary for the four layers within the following ranges: 300-600 m/s in the 1st layer; 200-1500 m/s in the 2nd and 3rd layers; 200-2400 m/s in the final half-space. Finally, the layer thickness ranges were chosen according to inspection of the geological map (see section A5.2) as follows: 5-15 m in the 1st layer; 15-20 m in the 2nd layer; 5-10 m in the 3rd layer.

In the inversion processing, velocity profiles are randomly generated within the given intervals for V_P , V_S , density and Poisson ratio. Then for each tested velocity model the forward computation of theoretical dispersion and HVSR curves is carried out. The misfit value is calculated as the summation at the sampled frequencies of the mean squared difference between theoretical and experimental values of the two curves.



Since obtained misfit values are reasonably low (<0.4 for the best-fit model) we consider this to be a good fit between experimental and theoretical curves. In Figure 15 we show the comparison between the theoretical HVSR and dispersion curves together with the experimental ones, which were the targets of the inversion procedure. Tested models with misfit lower than 0.49 are also shown in Figure 15. The color scale is related to the misfit value associated with each model.

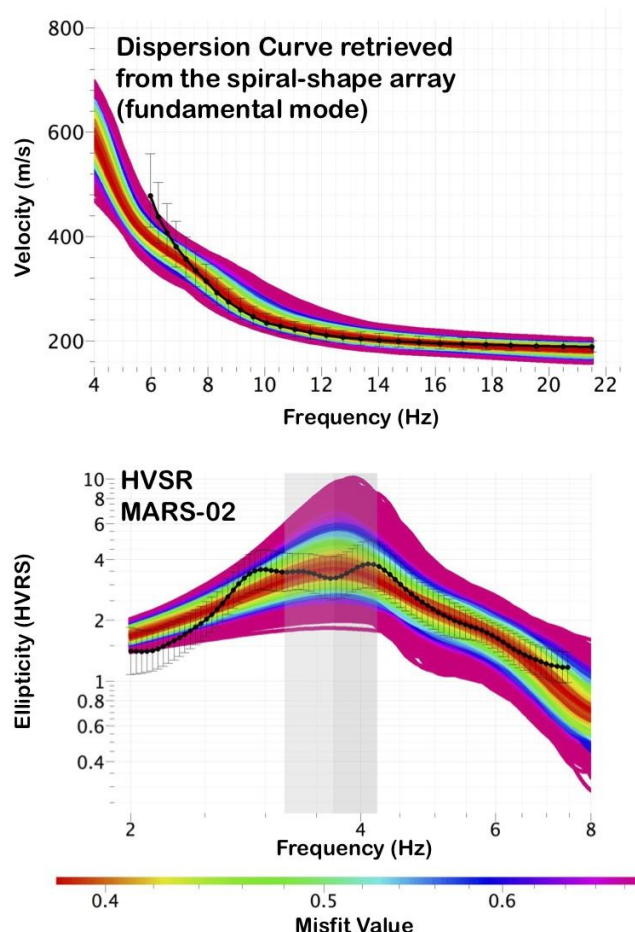


Figure 14. Theoretical dispersion (left panel) and HVSR curves (right panel), the color of each one being related to the model-associated misfit value (the color scale is shown at the bottom). Experimental curves, that were targets of the inversion procedure, are reported as well, together with their standard deviation (superimposed black curves and vertical bars).

Table 1

From	To	Thickness (m)	Vp (m/s)	Vs (m/s)	ρ (g/cm ³)	Description
0	0,4	0,4	318	142	1,7	Alluvial deposits
0,4	1,2	0,8	347	157	1,7	Alluvial deposits
1,2	2,7	1,5	388	178	1,7	Alluvial deposits
2,7	5,7	3,0	441	205	1,7	Alluvial deposits
5,7	11,8	6,1	508	240	1,8	Alluvial deposits

Convenzione DPC-INGV 2019-21, All.B2- WP1, Task 2: "Caratterizzazione siti accelerometrici" (Coord.: G.Cultrera, F. Pacor)

Cite as: Working group INGV "Agreement DPC-INGV 2019-21, All.B2- WP1, Task 2", (2020). Site characterization report at the seismic station IT.TVL - Tivoli (RM) <http://hdl.handle.net/2122/14053>



11,8	31,6	19,8	887	466	1,8	Volcanic deposits
31,6	41,4	9,8	1130	485	1,8	Volcanic deposits

1933 873 2,0

Seismic bedrock

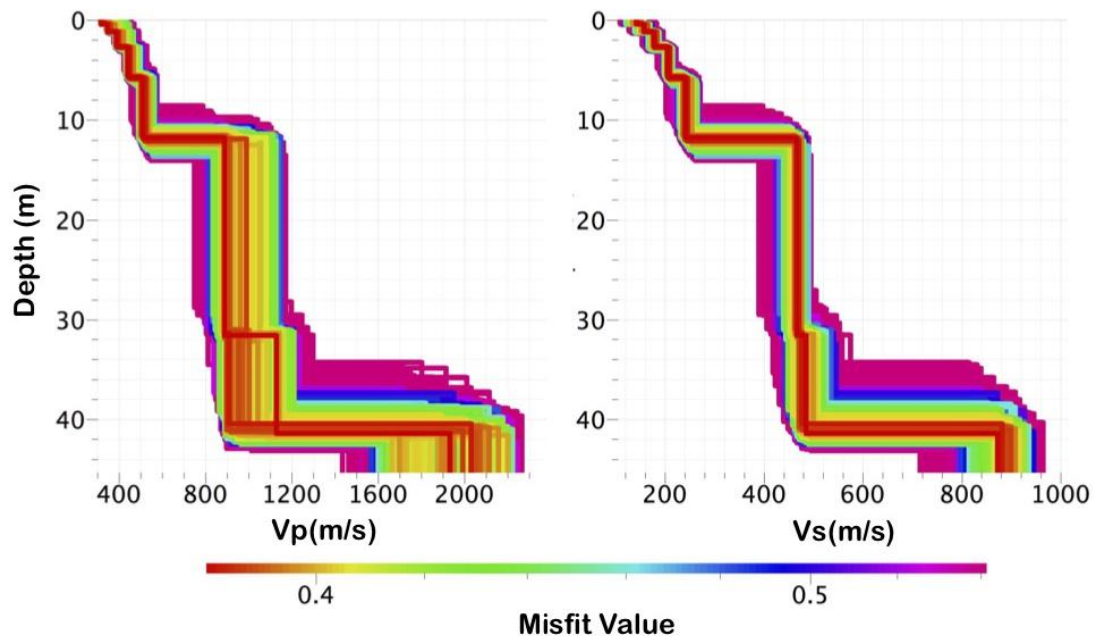


Figure 15. Tested models (with misfit up to 0.54). The color of each one is related to the associated misfit value.

The best-fit velocity model is shown in Figure 16. It is composed of three layers over the bedrock. The first one corresponds to the alluvial deposits (about 12 m thick) with V_p and V_s increasing from 318 to 507 m/s and from 142 to 240 m/s, respectively. The second and third layers are related to volcanic deposits, with similar mechanical properties and V_p ranging from 887 and 1130 m/s, and V_s ranging from 466 and 485 m/s. Finally, at about 42 meters we identify seismic bedrock, with velocities increasing to 1933 and 873 m/s for V_p and V_s respectively. This latter abrupt change of mechanical properties is most likely responsible of the 3.7 Hz peak revealed from the HVSR curve.

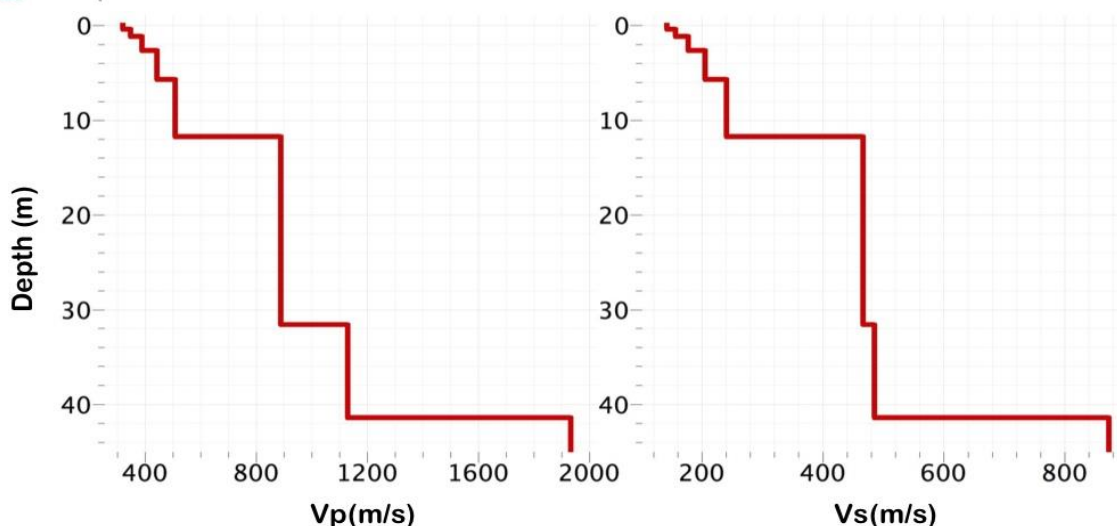


Figure 16. Best-fit model (misfit value of 0.382).

B3. CONCLUSIONS

Surface-wave analysis at IT.TVL station indicates that the site can be related to soil class-C, as prescribed in the Italian seismic design codes NTC-18 and NTC-08, and in the EC8 (Table 2). The best V_p and V_s models (i.e. lowest misfit) resulting from the inversion are shown in Figure 16 and Table 1. The HVSR of the temporary stations installed during the survey, show a clear peak at 3.9 Hz, that is consistent with the HVRS calculated at station IT.TVL using earthquake recording and published in the ITACA database (http://itaca.mi.ingv.it/ItacaNet_31/#/station/IT/TVL).

The passive spiral-shape array of geophones provided a reliable final dispersion curve from 6 to 21 Hz (Figure 13), and the inversion procedure resulted in the V_s models shown in Figures 15 and 16, the seismic bedrock being found at about 42 m (Table 1).

The V_{s30} retrieved from the best-fit model is 315.1 m/s (Table 2), therefore the station is classified following EC8 or NTC08 as soil class C. Following the definition of $V_{s,eq}$ within NTC18, since the value of 800 m/s is reached at a depth larger than 30 m, $V_{s,eq}$ is equal to V_{s30} and the site can be still related to class C. We highlight that this site was classified as B also in the Itaca database, where in absence of direct velocity measurements the site classification was assigned considering the outcropping lithotypes.

Table 2. f_0 value, and soil class following NTC08 and NTC18.

f_0 (Hz)	Note
3.9 Hz	The HVSR peak is almost isotropic

V_{s30} (NTC08 or EC8)	Soil Class
315.5 m/s	C

$V_{s,eq}$ (NTC18)	Soil Class
315.5 m/s	C



REFERENCES

Carta Geologica d'Italia in scala 1:100.000 (1943) - Foglio 150 - Roma. ISPRA
http://193.206.192.231/carta_geologica_italia/tavoletta.php?foglio=150

Carta Geologica d'Italia in scala 1:50.000 (in press) - Foglio 375 - Tivoli. ISPRA
https://www.isprambiente.gov.it/Media/carg/375_TIVOLI/Foglio.html

Commissione Tecnica per la Microzonazione Sismica (2015). Microzonazione sismica. Standard di rappresentazione e archiviazione informatica, Versione 4.0b (Commissione tecnica inter-istituzionale per la MS nominata con DPCM 21 aprile 2011)

Danese E. & Mattei M. (2010) - The sedimentary substrate of the Colli Albani volcano. In: Funiciello, R. & Giordano, G. (eds) The Colli Albani Volcano. Special Publication of IAVCEI, 3. The Geological Society, London, 000141-151000.

De Rita D., Faccenna C., Funiciello R. & Rosa. C. (1995) - Stratigraphy and volcano-tectonics. In: Trigila R. (A cura di): «The Volcano of the Alban Hills», Tipografia Sgs Roma: 33-71.

EN 1998-5 (2004). Eurocode 8: Design of structures for earthquake resistance - Part 5: Foundations, retaining structures and geotechnical aspects, CEN European Committee for Standardization, Bruxelles, Belgium.

Funiciello R. & Giordano, G. (a cura di) (2010) - The Colli Albani Volcano. Special Publication of IAVCEI, 3. The Geological Society, London, 401pp.

Funiciello R. & Parotto M. (1978) - Il substrato sedimentario nell'area dei Colli Albani: considerazioni geodinamiche e paleogeografiche sul margine tirrenico dell'Appennino centrale. Geologica Romana. 17: 233-287.

Giordano G., De Benedetti A.A., Diana A., Diano G., Gaudioso F., Marasco F., Miceli M., Mollo S., Cas R.A.F. & Funiciello R. (2006) - The Colli Albani caldera (Roma, Italy): stratigraphy, structure and petrology. In: R.A.F. Cas & G. Giordano (A cura di): «Explosive Mafic Volcanism», J. Volcanol. Geotherm. Res., Spec. Vol. 155: 49-80.

Giordano G., Mattei M. & Funiciello R. (2010) - Geological map of the Colli Albani volcano. In: Funiciello, R. & Giordano, G. (eds) The Colli Albani Volcano. Special Publication of IAVCEI, 3. The Geological Society, London. Insert.



Konno, K., Ohmachi, T., 1998. Ground-motion characteristics estimated from spectral ratio between horizontal and vertical components of microtremor. Bull. Seismol. Soc. Am. 88, 228e241.

Luzi L, Pacor F, Puglia R (2019). Italian Accelerometric Archive v3.0. Istituto Nazionale di Geofisica e Vulcanologia, Dipartimento della Protezione Civile Nazionale. doi: 10.13127/itaca.3.0.

Norme Tecniche per le Costruzioni (NTC08). Ministero delle Infrastrutture e dei Trasporti (2008). Decreto Ministero Infrastrutture. GU Serie Generale n. 29 del 04-02-2008 - Suppl. Ordinario n. 30.

Norme Tecniche per le Costruzioni (NTC18). Ministero delle Infrastrutture e dei Trasporti (2018). Decreto Ministero Infrastrutture. GU Serie Generale n. 42 del 20-02-2018 – Suppl. Ordinario n. 8.

Regione Lazio – Geoportale - <https://geoportale.regione.lazio.it/geoportale/>

Regione Lazio - Studio di Microzonazione Sismica di I Livello del Comune di Gallicano nel Lazio
http://www.regione.lazio.it/binary/prl_ambiente/tbl_sismicita/AMB_UAS_RM_Gallicano_nel_Lazio_MOPS_TAV_01.pdf

Sambridge, M., 1999. Geophysical inversion with a neighbourhood algorithm: I. Searching a parameter space. Geophys. J. Int. 138, 479e494.

Wathelet, M., Jongmans, D., Ohrnberger, M., 2005. Direct inversion of spatial autocorrelation curves with the neighborhood algorithm. Bull. Seismol. Soc. Am. 95, 1787e1800.



Disclaimer and limits of use of information

The INGV, in accordance with the Article 2 of Decree Law 381/1999, carries out seismic and volcanic monitoring of the Italian national territory, providing for the organization of integrated national seismic network and the coordination of local and regional seismic networks as described in the agreement with the Department of Civil Protection.

INGV contributes, within the limits of its skills, to the evaluation of seismic and volcanic hazard in the Country, according to the mode agreed in the ten-year program between INGV and DPC February 2, 2012 (Prot. INGV 2052 of 27/2/2012), and to the activities planned as part of the National Civil Protection System. In particular, this document¹ has informative purposes concerning the observations and the data collected from the monitoring and observational networks managed by INGV.

INGV provides scientific information using the best scientific knowledge available at the time of the drafting of the documents produced; however, due to the complexity of natural phenomena in question, nothing can be blamed to INGV about the possible incompleteness and uncertainty of the reported data.

INGV is not responsible for any use, even partial, of the contents of this document by third parties and any damage caused to third parties resulting from its use.

The data contained in this document is the property of the INGV.

Esclusione di responsabilità e limiti di uso delle informazioni

L'INGV, in ottemperanza a quanto disposto dall'Art. 2 del D.L. 381/1999, svolge funzioni di sorveglianza sismica e vulcanica del territorio nazionale, provvedendo all'organizzazione della rete sismica nazionale integrata e al coordinamento delle reti sismiche regionali e locali in regime di convenzione con il Dipartimento della Protezione Civile.

L'INGV concorre, nei limiti delle proprie competenze inerenti la valutazione della Pericolosità sismica e vulcanica nel territorio nazionale e secondo le modalità concordate dall'Accordo di programma decennale stipulato tra lo stesso INGV e il DPC in data 2 febbraio 2012 (Prot. INGV 2052 del 27/2/2012), alle attività previste nell'ambito del Sistema Nazionale di Protezione Civile.

In particolare, questo documento¹ ha finalità informative circa le osservazioni e i dati acquisiti dalle Reti di monitoraggio e osservative gestite dall'INGV.

L'INGV fornisce informazioni scientifiche utilizzando le migliori conoscenze scientifiche disponibili al momento della stesura dei documenti prodotti; tuttavia, in conseguenza della complessità dei fenomeni naturali in oggetto, nulla può essere imputato all'INGV circa l'eventuale incompletezza ed incertezza dei dati riportati.

L'INGV non è responsabile dell'utilizzo, anche parziale, dei contenuti di questo documento da parte di terzi e di eventuali danni arrecati a terzi derivanti dal suo utilizzo.

La proprietà dei dati contenuti in questo documento è dell'INGV.



This document is licensed under License

Attribution – No derivatives 4.0 International (CC BY-ND 4.0)

¹This document is level 3 as defined in the "Principi della politica dei dati dell'INGV (D.P. n. 200 del 26.04.2016)"

RESONANCE FREQUENCY

fo +/- STD [Hz]

Quality index 1

Source	Earthquake	Ambient noise	X																								
Ambient noise <table border="1"> <tr> <td>Method</td> <td>H/V</td> <td>X</td> <td>Ellipticity</td> <td>Other</td> </tr> <tr> <td>fo +/- std [Hz]</td> <td>3.9 +/- 0.43</td> <td></td> <td></td> <td></td> </tr> <tr> <td>Experiment date [DD/MM/YY]</td> <td>Distance from station [m]</td> <td>Lat. [WGS84]</td> <td>Lat. [WGS84]</td> <td></td> </tr> <tr> <td colspan="5">41.893069</td> </tr> </table>				Method	H/V	X	Ellipticity	Other	fo +/- std [Hz]	3.9 +/- 0.43				Experiment date [DD/MM/YY]	Distance from station [m]	Lat. [WGS84]	Lat. [WGS84]		41.893069								
Method	H/V	X	Ellipticity	Other																							
fo +/- std [Hz]	3.9 +/- 0.43																										
Experiment date [DD/MM/YY]	Distance from station [m]	Lat. [WGS84]	Lat. [WGS84]																								
41.893069																											
Environment <table border="1"> <tr> <td>Weather conditions</td> <td>Sunny</td> <td>Windy</td> <td>Rain</td> </tr> <tr> <td></td> <td colspan="3">X</td> </tr> <tr> <td>Soil sensor coupling</td> <td>Earth</td> <td>Asphalt</td> <td>Artificial</td> </tr> <tr> <td></td> <td colspan="3">X</td> </tr> <tr> <td>Urbanization</td> <td>None</td> <td>Dense</td> <td>Scattered</td> </tr> <tr> <td></td> <td colspan="3">X</td> </tr> </table>				Weather conditions	Sunny	Windy	Rain		X			Soil sensor coupling	Earth	Asphalt	Artificial		X			Urbanization	None	Dense	Scattered		X		
Weather conditions	Sunny	Windy	Rain																								
	X																										
Soil sensor coupling	Earth	Asphalt	Artificial																								
	X																										
Urbanization	None	Dense	Scattered																								
	X																										
Equipment <table border="1"> <tr> <td>Sensor</td> <td>Type [acc/vel]</td> <td>manufacturer</td> <td>cut off frequency [Hz]</td> </tr> <tr> <td>Digitizer</td> <td>Type</td> <td>Manufacturer</td> <td>Sampling frequency [Hz]</td> </tr> <tr> <td></td> <td colspan="3">Lennartz/Sara</td> </tr> <tr> <td>Measurement</td> <td>Number</td> <td colspan="2">Duration [min]</td> </tr> </table>				Sensor	Type [acc/vel]	manufacturer	cut off frequency [Hz]	Digitizer	Type	Manufacturer	Sampling frequency [Hz]		Lennartz/Sara			Measurement	Number	Duration [min]									
Sensor	Type [acc/vel]	manufacturer	cut off frequency [Hz]																								
Digitizer	Type	Manufacturer	Sampling frequency [Hz]																								
	Lennartz/Sara																										
Measurement	Number	Duration [min]																									
Analysis <table border="1"> <tr> <td>Software</td> <td>Fo uncertainty estimate from</td> </tr> <tr> <td>Smoothing type (e.g. triangular, Konno Ohmachi, ...)</td> <td>Fo from individual windows</td> </tr> <tr> <td></td> <td>H/V curve width</td> </tr> <tr> <td></td> <td>Manual picking</td> </tr> </table>				Software	Fo uncertainty estimate from	Smoothing type (e.g. triangular, Konno Ohmachi, ...)	Fo from individual windows		H/V curve width		Manual picking																
Software	Fo uncertainty estimate from																										
Smoothing type (e.g. triangular, Konno Ohmachi, ...)	Fo from individual windows																										
	H/V curve width																										
	Manual picking																										

Earthquake <table border="1"> <tr> <td>Method</td> <td>HVSR</td> <td>SSR</td> <td>GIT</td> <td>Other</td> </tr> <tr> <td>fo +/- std [Hz]</td> <td></td> <td></td> <td></td> <td></td> </tr> </table>		Method	HVSR	SSR	GIT	Other	fo +/- std [Hz]																					
Method	HVSR	SSR	GIT	Other																								
fo +/- std [Hz]																												
<table border="1"> <tr> <td>Recording period [DD/MM/YY]</td> <td>Number of earthquakes</td> <td>Epicentral distance [km]</td> <td>Magnitude range</td> </tr> <tr> <td>from</td> <td>to</td> <td>from</td> <td>to</td> </tr> </table>		Recording period [DD/MM/YY]	Number of earthquakes	Epicentral distance [km]	Magnitude range	from	to	from	to																			
Recording period [DD/MM/YY]	Number of earthquakes	Epicentral distance [km]	Magnitude range																									
from	to	from	to																									
HVSR <table border="1"> <tr> <td>Seismic phase</td> <td>P</td> <td>S</td> <td>Coda</td> <td>S + coda</td> <td>All</td> <td>window duration [s]</td> <td>Min</td> <td>Max</td> </tr> <tr> <td></td> <td colspan="5"></td> <td></td> <td></td> <td></td> </tr> </table>		Seismic phase	P	S	Coda	S + coda	All	window duration [s]	Min	Max																		
Seismic phase	P	S	Coda	S + coda	All	window duration [s]	Min	Max																				
SSR <table border="1"> <tr> <td>Seismic phase</td> <td>P</td> <td>S</td> <td>Coda</td> <td>S + coda</td> <td>All</td> <td>window duration [s]</td> <td>Min</td> <td>Max</td> </tr> <tr> <td></td> <td colspan="5"></td> <td></td> <td></td> <td></td> </tr> <tr> <td>Reference station</td> <td colspan="2">Lat. (WGS84)</td> <td colspan="2">Lon. (WGS84)</td> <td></td> <td></td> <td></td> <td></td> </tr> </table>		Seismic phase	P	S	Coda	S + coda	All	window duration [s]	Min	Max										Reference station	Lat. (WGS84)		Lon. (WGS84)					
Seismic phase	P	S	Coda	S + coda	All	window duration [s]	Min	Max																				
Reference station	Lat. (WGS84)		Lon. (WGS84)																									
GIT <table border="1"> <tr> <td>Parameters</td> <td colspan="3">Free (to be inverted)</td> <td>Imposed</td> </tr> <tr> <td></td> <td colspan="3"></td> <td></td> </tr> <tr> <td>Reference paper</td> <td colspan="3"></td> <td></td> </tr> <tr> <td>Reference station</td> <td>Lat. (WGS84)</td> <td>Lon (WGS84)</td> <td></td> <td></td> </tr> </table>		Parameters	Free (to be inverted)			Imposed						Reference paper					Reference station	Lat. (WGS84)	Lon (WGS84)									
Parameters	Free (to be inverted)			Imposed																								
Reference paper																												
Reference station	Lat. (WGS84)	Lon (WGS84)																										

Vs30

Vs30 +/- STD [m/s]

Quality index 1

Source	Geophysical measurements	X Geotechnical measurements	Digital Elevation Model (DEM)	Geology	DEM & Geology
--------	--------------------------	-----------------------------	-------------------------------	---------	---------------

Geophysical measurements

Method	Surface waves methods (active, passive methods)	Borehole methods (DH, CH, PS Logging)
Vs30 +/- STD [m/s]	From Vs(z)	X From Down Hole
	From Vr40	From Cross Hole
	From Vs _z Vs30 correlation	From PS Logging
Reference relationship		
Vs _z Vs30		

Geotechnical measurements

Method	N SPT	CPT	Shear strength	OTHER
Vs30 +/- STD [m/s]				
Experiment date [DD/MM/YY]	Distance from station [m]	Lat. [WGS84]	Lon. [WGS84]	

Reference relationship	N-SPT
Vs30 geotechnical parameter	CPT
	Shear strength
	Other

Geology

Method	Geological map	Stratigraphic log
Vs30 +/- STD [m/s]		
Geological map scale		
Geological unit name		
Stratigraphic log	Experiment date [DD/MM/YY]	Lat. [WGS84] Lon. [WGS84]
Reference relationship		
Vs30 geology		
Reference relationship		
Vs30 Stratigraphic log		

Digital Elevation Model

Vs30 +/- STD [m/s]	
DEM resolution	
Reference relationship	
Slope Vs30	

Slope range	from
	to

DEM & GEOLOGY

Vs30 +/- STD [m/s]	
Reference relationship Slope	
Vs30 geology	

Vs profile

Quality index 1

Source	Non invasive methods (active and/or passive seismics)			Invasive methods (measurement in borehole)
	Active surface waves	Refraction		
	Passive surface waves	X	Refraction	
	HV / ellipticity			PS-Logging

Non invasive : surface waves methods

Experiment date [DD/MM/YY]	Distance from station [m]		Lat. [WGS84] center location	Lon. [WGS84] center location
	Min	Max		

Active surface waves acquisition layout

Minimum receiver spacing (m)
Profile length (m)*
Geophones number
Number of profiles

* Provide the length for the various profiles (e.g. 46 m, 94 m)

Geophone cut-off frequency (Hz)
Geophone type (vertical / horizontal)
Geophone manufacturer
Source (hammer, vibrator, ...)
Digitizer type
Digitizer manufacturer

Weather conditions	Sunny	Windy	Rain	Soil sensor coupling	Earth	Asphalt	Artificial	Urbanization	None	Dense	Scattered
--------------------	-------	-------	------	----------------------	-------	---------	------------	--------------	------	-------	-----------

Passive surface waves acquisition layout

Number of sensors
Minimum array aperture
Maximum array aperture
Number of arrays
Minimum duration [min]

Sensor cut-off frequency (Hz)
Sensor type (vertical / horizontal)
Sensor manufacturer
Digitizer type
Digitizer manufacturer

Weather conditions	Sunny	Windy	Rain	Soil sensor coupling	Earth	Asphalt	Artificial	Urbanization	None	Dense	Scattered
	x				x				x		

Type of dispersion and/or H/V estimates

Rayleigh DC	x	Reference paper (Name, Journal, DOI)
Love DC		
Ellipticity	x	
H/V (DFA, EHVR)		
H/V (SH)		

Dispersion curves

Rayleigh	Love
Min wavelength (m)	
Max. wavelength (m)	
Min. phase vel. (m/s)	
Max. phase vel. (m/s)	
Modes (R0, L0, ...)	

H/V or Ellipticity curves

Min. frequency (Hz)	Max. frequency (Hz)
---------------------	---------------------

Inversion

Rayleigh waves	x	Love waves	Ellipticity curves	x	H/V (DFA, EHVR)	H/V (SH)	resonance frequency
A priori information used in inversion		seismic refraction			stratigraphic log	geotechnical information	water table depth
Inversion algorithm/code							
Reference							

Non invasive : body waves methods

Experiment date [DD/MM/YY]	Distance from station [m]		Lat. [WGS84] center location	Lon. [WGS84] center location
	Min	Max		

Acquisition layout

Receiver spacing (m)	Geophone cut-off frequency (Hz)
Profile length (m)*	Geophone type (vertical / horizontal)
Geophones number	Geophone manufacturer
Number of profiles	Source (hammer, vibrator, ...)
Shot spacing (m) - reflection meas.	Digitizer type
	Digitizer manufacturer

* Provide the length for the various profiles (e.g. 46 m, 94 m)

Weather conditions	Sunny	Windy	Rain	Soil sensor coupling	Earth	Asphalt	Artificial	Urbanization	None	Dense	Scattered
--------------------	-------	-------	------	----------------------	-------	---------	------------	--------------	------	-------	-----------

Processing methods

	Reference paper (Name, Journal, DOI)
classical refraction	
refraction tomography	
classical reflection	
advanced method	

Invasive methods

OTHER

Down Hole Cross Hole PS Logging SPT CPT

Borehole depth (m)
Geophone type
Source type
Distance between wells
Depth resolution (m)
Latitude (WGS84)
Longitude (WGS84)
Distance from station (m)
P-wave velocity
S-wave velocity

Processing methods

Reference paper (Name, Journal, DOI) or ASTM norm

Down-Hole
Cross-Hole
PS-Logging
SPT
CPT
OTHER

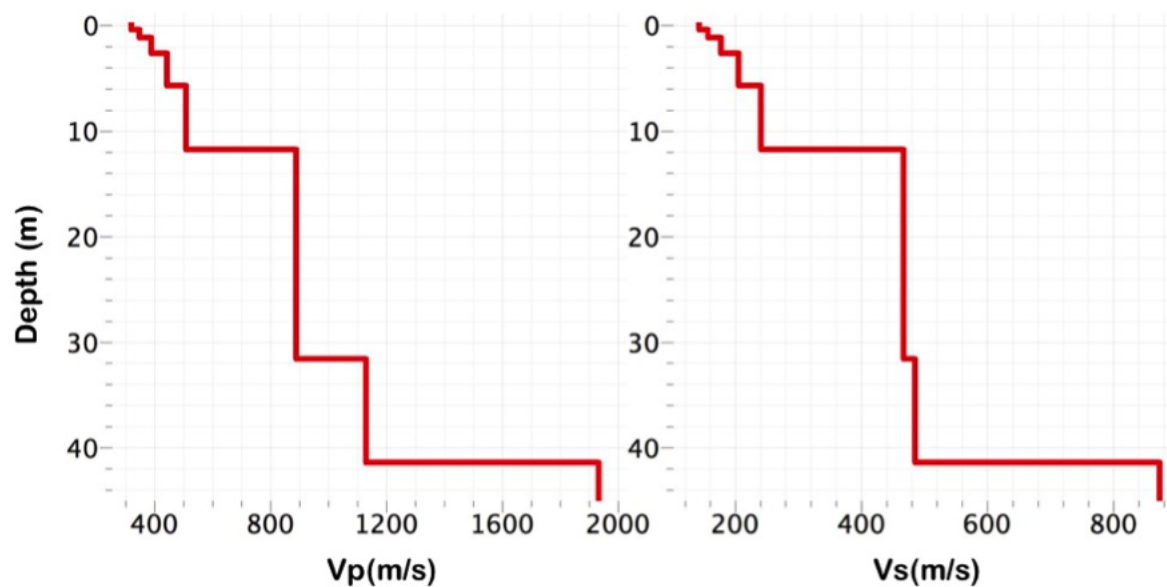
Authoritative velocity profile

Note: You do not have to fill in all the columns. You can provide either single values for Vp or Vs (e.g. profiles derived from borehole measurements) or either a range for Vp and Vs (e.g. profiles derived from stochastic surface waves inversion)

Is Vs derived from Vp ?		Yes	No	x					
Top depth (m)	Bottom depth (m)	Vp (m/s)	STD Vp (m/s)	Vs (m/s)	STD Vs (m/s)	Vs min (m/s)	Vs max (m/s)	Vp min (m/s)	Vp max (m/s)

x

Figure with authoritative velocity profiles



Surface geology

Quality index 1

Source	Cartography (geological, lithological, ...)
--------	---

Field survey

Stratigraphic log

Geological map

Map reference	
Map scale	
Map sheet	
Predominant geologic/lithologic unit	Name : Description : Age : Thickness : Rock mass structure :
Fault presence	
Weathering	
Cross section	

Field survey

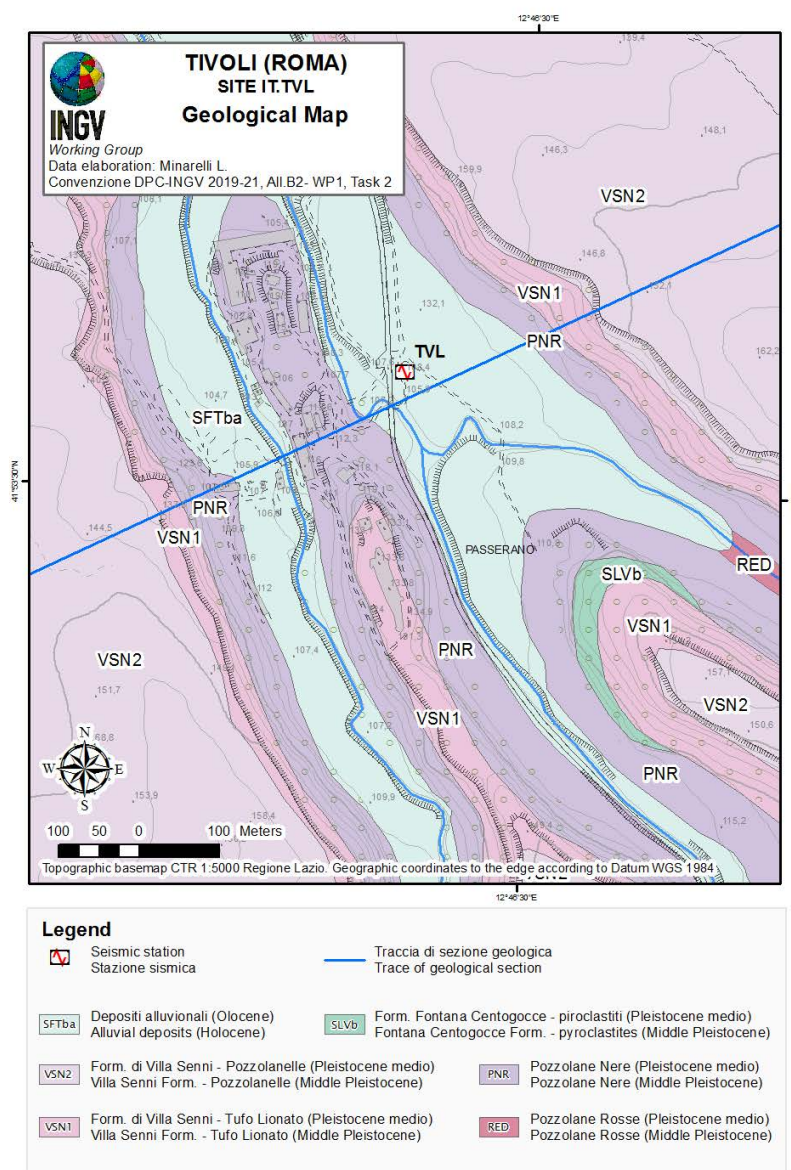
Map reference	
Map scale	
Predominant geologic/lithologic unit	Name : Description : Age : Thickness : Rock mass structure :
Fault presence	
Weathering	
Cross section	

Stratigraphic log

log depth (m)		
Top depth (m)	Bottom depth (m)	Stratigraphic description

Surface geology

Map



Site class

Site class
Quality index 1

Reference building code for site classification (EC8 1, EC8 2, NEHRP, national code, ...)	
--	--

Source	Geophysical measurements	x	Geotechnical measurements	Digital Elevation Model (DEM)	Geology	DEM & Geology
--------	--------------------------	---	---------------------------	-------------------------------	---------	---------------

Reference relationship geology soil class
Reference relationship slope from DEM soil class
Reference relationship slope from DEM geology soil class

Parameters for deriving soil class as prescribed in building code

Seismological bedrock depth

Depth +/- STD [m]
Quality index 1



Vs profile

	Non invasive methods	Invasive seismic methods	Geotechnical methods
Bedrock depth +/- STD(m)			
Bedrock Vs +/- STD(m)			
Bedrock Vp +/- STD(m)			
Is Vs derived from Vp ?	Yes	No	x

Resonance frequency

Bedrock depth +/- STD(m)
Reference relationship Fo
bedrock depth

Geology

Bedrock depth +/- STD(m)
Bedrock geological unit
Reference

Stratigraphic log

Bedrock depth +/- STD(m)
Bedrock geological unit
Reference

Other methods

Bedrock depth +/- STD(m)	Reference
Gravity	
Seismic refraction	
Seismic reflection	
TDEM	

Engineering bedrock depth

Depth +/- STD [m]

Quality index 1

Reference Vs related to
engineering bedrock in m/s

Reference building code for site classification
(EC8 1, EC8 2, NEHRP, national code, ...)

Source

Vs profile

x

Geology

Stratigraphic log

Vs profile

	Non invasive methods	Invasive seismic methods	Geotechnical methods
Bedrock depth +/- STD(m)			

Is Vs derived from Vp ?

Yes

No

x

Geology

Bedrock depth +/- STD(m)
Bedrock geological unit
Reference

Stratigraphic log

Bedrock depth +/- STD(m)
Bedrock geological unit
Reference